Compact Denatured State of a Staphylococcal Nuclease Mutant by Guanidinium As Determined by Resonance Energy Transfer†

E. James, P. G. Wu, W. Stites, and L. Brand*

Department of Biology, The Johns Hopkins University, Baltimore, Maryland 21218

Received June 23, 1992; Revised Manuscript Received August 5, 1992

ABSTRACT: The protein from a mutant clone of staphylococcal nuclease with a cysteine substituting for a lysine at position 78 was prepared and labeled with a cysteine-specific fluorescent probe 5-[[2-[(iodoacetyl)-amino]ethyl]amino]naphthalene-1-sulfonic acid (IAEDANS). Time-resolved nonradiative energy-transfer studies were done using the single tryptophan at position 140 as the energy donor and the IAEDANS as the receptor. Changes in distance and distance distributions were observed as a function of increasing guanidinium (GuHCl) concentration (0–2 M) and in the presence or absence of Ca^{2+} and inhibitor 2′-deoxythymidine 3′,5′-diphosphate (pdTp). In the native state, both the ternary complex and the noncomplexed protein are best fit with one population having an average donor–acceptor distance of ~23 Å and an "apparent" full width at half-maximum (fwhm) of distance distribution of ~18 Å. Besides the contribution of linker arm of the acceptor, it appears that there are some conformational heterogeneties either due to the disordering of the tryptophan region or due to the whole protein in the native state. During GuHCl unfolding, the average distance remains relatively constant up to GuHCl concentrations where both the ternary complex and the ligand-free protein are denatured (1–1.3 M). The compact denatured states persist up to 2 M GuHCl. At 2 M GuHCl, the heterogeneity of the denatured state in the ternary complex is much larger than that of the ligand-free nuclease. The results show that the denatured states of staphylococcal nuclease mutant K78C by GuHCl are compact and these compact denatured states are likely due to residual structures or incompletely disrupted hydrophobic cores under these conditions.

A time-resolved resonance energy-transfer method has been used to obtain distance and distance distributions in proteins (Amir & Haas, 1986; Lakowicz et al., 1988; Haas et al., 1988; Albaugh & Steiner, 1989) under native or denaturing conditions. This method can give long-range distance and distance distribution in a single measurement and is quite applicable to the study of protein folding (Haas et al., 1988; Lakowicz et al., 1988).

Staphylococcal nuclease is a single-domain protein with no disulfide bonds. It consists of 149 amino acids with only a single tryptophan located at position 140. It has been extensively studied and used as a model for protein folding (Anfinsen, 1973). The equilibrium unfolding of the nuclease has been approximated by a two-state model, and the changes in fluorescence emission of Trp 140 have been shown to correspond to changes in the protein secondary structure and mimic the cooperative unfolding of the protein (Anfinsen et al., 1972; Shortle & Meeker, 1986). Recent work by Shortle and co-workers (Shortle & Meeker, 1986; Shortle et al., 1990) using site-directed mutagenesis has revealed many factors governing the stability of the nuclease.

In this work, we used a staphylococcal nuclease mutant, K78C, where lysine at position 78 was replaced by a cysteine, to estimate the distance distribution between tryptophan 140 and cysteine 78 by resonance energy transfer. The substitution by a cysteine allows site-specific labeling of the nuclease mutants (Beechem et al., 1990). The Cys 78 was labeled by a cysteine-specific fluorescent probe, 5-[[2-[(iodoacetyl)-amino]ethyl]amino]naphthalene-1-sulfonic acid (IAEDANS),[1] which was used as an energy acceptor from donor fluorescence of Trp 140. The following questions are to be addressed: (1) what is the overall dimension of the protein in the denatured state? (2) How does the binding of Ca^{2+} and pdTp affect the distance distribution in the native and denatured states of the nuclease? (3) How does the binding of Ca^{2+} and pdTp affect the pathway from native to denatured states?

In the text following, we operationally designate the equilibrium state immediately after the cooperative breakdown of the protein as the "denatured" state, which may not necessarily be in an unfolded state devoid of any regular secondary structures. In fact, some proteins have residual structures in the denatured state (Tsong, 1975). The designation of denatured state is consistent with that proposed by Shortle (1989) and is consistent with the terminology used with nuclease. As will be shown later, denatured staphylococcal nuclease does possess some structures and thus the denatured state(s) of the nuclease can be considered as some early intermediate(s) in terms of folding/unfolding processes. It should be noted that the definition of denatured state by different measurements may be different. In many previous studies using other techniques, the physical properties of proteins at higher denaturant concentrations are indistinguishable from those immediately after the cooperative breakdown of the proteins. Thus the states of denatured proteins within a large range of denaturant concentrations were usually regarded as one denatured state with no structures present. As more techniques are applied to the problem of protein folding, more structural details of the denatured states

† Supported by NIH Grant GM 11632 (L.B.), NIH Training Grant 5T32 GM-07231 (E.J.), NSF Grant DIR-8721059 (P.G.W.), and NIH Grant GM 34171 (W.S. to D. Shortle).

* Corresponding author.

[1] Abbreviations: fwhm, full width at half-maximum height; pdTp, 2′-deoxythymidine 3′,5′-diphosphate; IAEDANS, 5-[[2-[(iodoacetyl)-amino]ethyl]amino]naphthalene-1-sulfonic acid; DTNB, 5,5′-dithiobis-(2-nitrobenzoic acid).

0006-2960/92/0431-10217$03.00/0

can be elucidated. Consequently the description of the denatured states become more complicated. On the other hand, protein denaturation may be described from a structural point of view as folded to unfolded states. Again the possible existence of partially folded states complicates the correlation between folding/unfolding and renaturation/denaturation.

MATERIALS AND METHODS

Protein Purification. The clone for staphylococcal nuclease K78C was isolated from a stab culture of *Escherichia coli* having the inducible plasmid pL9 containing the coding sequence for the nuclease gene and an ampicillin resistance gene as a selectable marker. The DNA sequence was altered to change the lysine at position 78 to a cysteine. The mutant was provided by D. Shortle (The Johns Hopkins University). The protein was prepared by the method of Shortle and Meeker (1989) up to the step of the ion exchange column. The nuclease was first purified by an ion exchange column (CM-25 carboxymethyl-Sephadex), which produced greater than 90% pure protein. The protein was further purified by a reactive green no. 5–agarose column (Sigma). The resin, which was a 4% cross-linked beaded agarose, was swollen in 0.1 M Tris, 25 mM $CaCl_2$, pH 7.5 at 4 °C, degassed, and poured into a column 2 cm × 10 cm. The column was equilibrated with the same buffer in 10 column volumes. The column was run at 4 °C. The protein was slowly loaded at a rate of 0.5 mL/min and washed with the same buffer. The contaminating protein was eluted in the void volume. The nuclease was eluted by 0.1 M Tris, 2 M NaCl, pH 7.8. Protein purity was accessed to be ~99% pure by silver-stained denaturing polyacrylamide gel electrophoresis and HPLC.

The concentration of wild-type nuclease was calculated using the molar absorption coefficient $\epsilon = 15\,630$ at 280 nm (Fuchs et al., 1967). The molar absorption coefficient of K78C (with the substitution of cysteine for a lysine) was calculated to be $\epsilon = 15\,770$ at 280 nm using the molar absorption coefficients of tryptophan, tyrosine, and cysteine which were obtained by linear least-squares fitting of the known molar absorption coefficients of the proteins listed by Gill and von Hippel (1989). The protein concentrations thus obtained are in good agreement with those from the Coomassie assay using wild-type nuclease as a standard. With the exception of the 5,5′-dithiobis(2-nitrobenzoic acid) (DTNB) titration and protein labeling, in all the other studies, the buffer solution used was 0.1 M Tris, 0.05 M NaCl, pH 7.8.

Protein Labeling and Characterization. The presence and reactivity of the cysteine in the nuclease was determined by titration of the protein sample with DTNB. The formation of TNB anion was monitored at 418 nm according to the procedure of Ellman (1959). The number of thiol groups per protein molecule was determined to be 1.0 ± 0.1 under denaturing conditions. The protein was only partially reactive under native conditions due to the presence of dimers.

The enzymatic activity of K78C was determined by monitoring the rate of change in the absorbence of calf thymus DNA at 260 nm as it is hydrolyzed by the nuclease (Cuatrecasas et al., 1967). The activity of both the unlabeled and labeled nuclease was determined in this manner and expressed as absorbance (Abs) per minute per milligram of protein. The activity of wild-type nuclease was about 1000–1200 Abs min^{-1} mg^{-1}. For the mutant, the activity of the unlabeled K78C was about 950–1200 Abs min^{-1} mg^{-1} and that of the labeled K78C was ~600 Abs min^{-1} mg^{-1}. The variation in activity assay was quite large, and the material of labeled protein was quite limited. Thus the results are only qualitative.

The labeling of the cysteine (dimers reduced) was done by reaction with the SH-specific probe 5-[[2-[(iodoacetyl)amino]-ethyl]amino]naphthalene-1-sulfonic acid (IAEDANS, Molecular Probes), under denaturing conditions, 5 M urea, 0.1 M Tris, 50 mM NaCl, pH 8.0. The IAEDANS was in a 10-fold molar excess relative to the cysteine concentration. The sample was stirred overnight in the dark at room temperature. Excess dye was removed from the labeled protein by dialysis followed by a Sephadex desalting column G-25 (Bio-Rad). The percent labeling is determined spectroscopically using the molar absorption coefficients $\epsilon = 6100$ at 337 nm and $\epsilon = 1060$ at 280 nm (Hudson & Weber, 1973) for IAEDANS and also by DTNB titration. Both methods showed that the protein was essentially 100% labeled. The fluorescence decay data were also consistent with full labeling. In the data analysis of energy transfer, we checked the decay data by including a percentage labeling parameter and the unlabeled was less than 5%, which is about within the noise of the experiments for this protein with a very wide distance distribution. Wild-type nuclease was used as a control, and no detectable nonspecific labeling was found.

The nuclease K78C was also labeled at the SH group by a bulky probe, biocytin iodoacetamide (Molecular Probes), which is not an energy acceptor for tryptophan. Thermal melting of the labeled and unlabeled proteins showed similar profiles as monitored by tryptophan fluorescence, indicating labeling of the proteins has not destabilized the protein to a detectable degree. Since IAEDANS is smaller than biocytin, the nuclease labeled with the energy-transfer acceptor IAEDANS is expected to be in its native form. Furthermore one titration data set of the energy-transfer sample as will be shown in the Results section follows exactly the denaturation curve of the unlabeled protein, implying the labeled protein is indeed in the native state.

Absorption and Steady-State Fluorescence Measurements. Absorption spectra were obtained using a Cary 219 spectrophotometer. Steady-state fluorescence measurements were made on an SLM 8000 photon-counting spectrofluorometer with protein concentration below 0.1 OD at 280 nm; buffer conditions, 0.1 M Tris, 0.05 M NaCl, pH 7.8. When used to calculated spectral overlaps, the emission spectra of free tryptophan and tryptophans in proteins were corrected with reference to *N*-acetyl-L-tryptophanamide, both in native buffer and in various Tris-buffered guanidinium chloride (GuHCl, pH 7.8) solutions. Tryptophan was excited at 295 nm, and IAEDANS at 340 nm. Emission was detected at the magic angle (54.7°) to eliminate polarization effects.

The quantum yield of tryptophan in the nuclease was determined in reference to free tryptophan with $\phi = 0.14$ in water at 25 °C (Kirby and Steiner, 1970). The total intensity of free tryptophans was measured at several concentrations, and these intensities vs concentrations were fitted to a straight line with the slope proportional to the quantum yield of tryptophan. Likewise, several protein concentrations were used to get the slope. With the ratio of the two slopes and the known quantum yield of free tryptophan, we then calculated the quantum yield of the nuclease. The quantum yields of the protein in various GuHCl concentrations were determined in the same way.

For the measurements of the ternary complex of nuclease K78C with calcium and 2′-deoxythymidine 3′,5′-diphosphate (pdTp, Pharmacia), $CaCl_2$ and pdTp solutions were added to a fresh sample of labeled K78C solution. The concentration of Ca^{2+} was 20 mM and that of pdTp 2 mM. Under these

conditons, the binding of ligands is saturated (Serpersu et al., 1986).

Time-Resolved Fluorescence Measurements. For energy-transfer experiments, the fluorescence decay of tryptophan in the nuclease was measured using a time-correlated single-photon-counting apparatus as described before (Badea & Brand, 1979) with a picosecond synchronously pumped mode-locked dye laser system (Spectra-Physics 3000 Series). The dye laser (Rodamine 6G) output at 590 nm was frequency-doubled to 295 nm. The emission was detected with a magic angle polarizer at an emission wavelength of 350 nm. A Ludox solution was used to collect the instrument response. The photomultiplier tube color effect was corrected with reference to melatonin in water, which has a single lifetime of ~5.4 ns. Equal time collections were carried out for sample and blank buffer when the intensity of the protein was low, as it is in the denatured state. Duplicate or triplicate data were collected at each GuHCl concentration. The samples were kept at 20 °C in a thermostated cuvette holder.

After the completion of the GuHCl titration, the labeled protein was checked for any change in percentage labeling by absorption and DTNB titration. It was still fully labeled.

Data Analysis. The fluorescence decay of the single tryptophan in staphylococcal nuclease mutant K78C was analyzed by a sum of exponentials when unlabeled.

$$I(t) = \sum_i \alpha_i \exp(-(t/\tau_i)) \qquad (1)$$

where α_i and τ_i are the amplitude and lifetime of the ith component. The impulse model function (1) was then convoluted with the measured instrumental response to get the calculated intensity decay $i_c(t)$, which was compared with the measured decay data $i(t)$. α_i and τ_i were then optimized by nonlinear least-squares methods. The goodness of the fit was judged by the reduced χ^2, which should be close to 1.0 for a good fit. For each fit we also used additional criteria. We plotted the weighted residuals and calculated the autocorrelation of the residuals (Grinvald & Steinberg, 1974) to make sure there were no systematic deviations (both should be random about zero).

The distance and distance distributions between Trp 140 and IAEDANS at position 78 were obtained by analyzing the change of tryptophan fluorescence decay due to nonradiative energy transfer. To analyze the fluorescence decay of Trp 140 in the presence of an acceptor IAEDANS, we used the following assumptions. (1) The critical or Förster transfer distance R_{0i} of each component is the same; i.e., $R_{0i} = R_0$. Since R_0 is almost always determined from steady-state spectral overlap of donor emission and acceptor absorption and from the quantum yield of the donor, both of which are averaged quantities, it is not very meaningful to reassign each decay component with a different R_0. Additionally, we have measured the decay-associated spectra of the protein; it appears that the spectral shapes of the two components in the native protein are about the same. As will be shown in the Results section, a scaled R_0 according to different lifetimes contributes little to the observed width of distance distribution. In any case, R_0 only affects the average distance and the uncertainties introduced to the distance distribution due to R_0 are much smaller than other factors. (2) κ^2 was assumed $^2/_3$. The amplitude associated with the IAEDANS motion (excited at 340 nm) when measured in native and denatured K78C showed little change, indicating the acceptor is free to rotate. On the other hand, there is some constraint on the Trp 140 in the native protein; its orientation cannot be totally random. Although its distribution is unknown, we can estimate the upper limit of its contribution to the distance distribution. (3) Some local rotational or translational diffusion between donor and acceptor may occur and was not included in the analysis. This gave a lower limit to the width of the distribution. The motions of donor and acceptor are coupled to the protein internal motions. Since we do not know whether the motion on the nanosecond scale is of a stationary type, which can be characterized by time-independent diffusion coefficients, or of a nonstationary type, which requires time-dependent diffusion coefficients, we have not attempted to analyze our data with diffusion. K78C labeled by an acceptor with a much shorter linker arm showed static orientational contribution to apparent distance distribution (Wu & Brand, 1992). Thus motions of donor and acceptor, even in the present case of a long linker arm, are limited to be local when the protein is in its native state or near its denatured state. Since we are comparing distance distributions with and without ligand binding, and as a function of GuHCl concentration, the absolute value of the distance itself is not required. The relative changes (differences) are the focus of this study. At higher GuHCl concentrations, the protein further unfolds to become random coils and diffusion may become more important. Due to the large reduction in tryptophan quantum yield when the protein is denatured, however, it is very difficult to use this donor–acceptor pair to extend the study far beyond the denaturing GuHCl concentration.

Given the amplitudes and lifetimes of the donor in the absence of acceptor as in eq 1, the fluorescence decay of the donor in the presence of an acceptor can be written as

$$I(t) = \sum_k a_k \int p_k(r) \sum_i \alpha_i \exp\left[-\frac{t}{\tau_i}\left(1 + \left(\frac{R_0}{r}\right)^6\right)\right] dr \qquad (2)$$

where the first sum refers to the number of distributions. a_k is the relative concentration of the kth population and $p_k(r)$ is the distance distribution probability [$\int p_k(r)\, dr = 1.0$].

We used a Gaussian form for the distribution as used by others (Haas et al., 1975; Lakowicz et al., 1988; Albaugh & Steiner, 1989) to describe the shape of the distance distribution

$$p(r) = \frac{1}{\sqrt{2\pi}\sigma} \exp\left[-\frac{1}{2}\left(\frac{r - \bar{r}}{\sigma}\right)^2\right] \qquad (3)$$

where $\bar{r}$ is the mean distance and σ is related to the full width at half-maximum height (fwhm) by fwhm = $2(2 \ln 2\sigma)^{1/2}$ = 2.355σ. fwhm characterizes the broadness of the distance distribution. It is important to note that when $\kappa^2 = {}^2/_3$ is used, the fwhm represents both the real distance distribution and the orientational distribution if the donor or acceptor rotations are slower than the fluorescence decay rates. While the use of $\kappa^2 = {}^2/_3$ is justified in the calculation of average distances (Wu & Brand, 1992), its use in distance distribution analysis of time-resolved decay data is only for convenience of calculation. Dispersion or distribution of any variable in the Förster equation could then be translated into an "apparent" distance distribution. Thus an "apparent" distance distribution could be due to real distance heterogeneity, orientational disorder, or linker arm of the probes. Both $\bar{r}$ and σ are adjustable parameters in the fitting of the donor–acceptor decay data. Identical to the case of donor-only decay, we used χ^2, residuals, and autocorrelation of the residuals to judge the goodness of the fit.

The critical transfer distance R_0 was calculated according to

$$R_0^6 = 8.78 \times 10^{-5} \frac{\phi \kappa^2}{n^4} \int F_D(\lambda) \epsilon_A(\lambda) \lambda^4 \, d\lambda \qquad (4)$$

where ϕ is the quantum yield of tryptophan in the absence of acceptor, $\kappa^2 = {}^2/_3$, and n is the index of refraction. $n = 1.4$ was used. $F_D(\lambda)$ is the normalized emission of the donor, and $\epsilon_A(\lambda)$ the absorption coefficient of the acceptor. Both the overlap integral and quantum yield change upon denaturation. The value of R_0 under native conditions was calculated to be 22.8 Å and that under denatured conditions to be 18.1 Å. For one data point in the middle of the transition we used R_0 = 20.0 Å.

The fluorescence decay of the donor–acceptor pair was also analyzed empirically by multiexponentials as in eq 1. This gave the average lifetime of the donor–acceptor pair $\langle \tau_{DA} \rangle$, compared to the case of donor-only, which gave the average lifetime of the donor $\langle \tau_D \rangle$. The average energy-transfer efficiency $\bar{E}$ was calculated by

$$\bar{E} = 1 - \langle \tau_{DA} \rangle / \langle \tau_D \rangle \qquad (5)$$

and the average distance (without distribution analysis) was calculated by

$$\bar{r} = R_0((1 - \bar{E})/\bar{E})^{1/6} \qquad (6)$$

This equation illustrates that the distance determined in energy-transfer measurements is referenced to R_0. Donor–acceptor pairs with different R_0's can be used to estimate distances of different ranges. Since both $\langle \tau_{DA} \rangle$ and $\langle \tau_D \rangle$ are obtained without the absolute protein concentrations, uncertainities associated with protein concentration determinations, especially in the case of labeled proteins, are eliminated by time-resolved fluorescence measurements.

The integration in eq 2 started from $0.4R_0$ to $2.2R_0$ in 0.1–0.2-Å steps. This covers distances at which energy-transfer efficiency varies from less than 0.5% to greater than 99.5%.

RESULTS

Denaturation of the Unlabeled K78C by GuHCl. The denaturation of mutant K78C by GuHCl is briefly described here. Figure 1A shows the steady-state fluorescence intensity of Trp 140 in the unlabeled protein as a function of GuHCl concentration in the absence and presence of Ca^{2+} and pdTp. Assuming a two-state denaturation, the equilibrium constant between native and denatured states can be calculated as (Shortle, 1986)

$$K = (I_N - I)/(I - I_D)$$

where I_N and I_D are the fluorescence intensities of the native and denatured states, respectively. The plot of ln K vs [GuHCl] is shown in the inset of Figure 1A for the nuclease with and without ligands. Both the plots are linear with correlation coefficients greater than 0.99 for the range of equilibrium denaturation constants, changing more than 1000-fold. The slopes relative to wild types are 0.93 (no calcium and pdTp) and 0.96 (with calcium and pdTp). We measured the entire spectrum of tryptophan emission at various GuHCl concentrations. For comparison with time-resolved data, we only showed the results at 350-nm emission. The plots at other wavelengths, such as at 320 nm, gave almost identical results for the nucleases with and without ligand binding. Thus it appears that this mutant, like the wild type and many other mutants as measured by fluorescence and circular

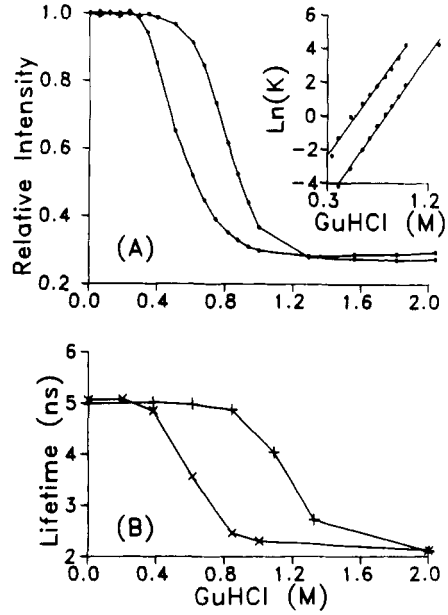

FIGURE 1: GuHCl denaturation of K78C. (A) Steady-state fluorescence intensity of Trp 140 (no labeling) as a function of [GuHCl] in the absence (left curve) and presence (right curve) of calcium and pdTp; excitation 295 nm, and emission 350 nm. Inset: equilibrium denaturation constant calculated from the intensities vs [GuHCl]. (B) Average lifetime of Trp 140 obtained from decay data vs [GuHCl] without (left curve) and with (right curve) calcium and pdTp; excitation 295 nm, and emission 350 nm. The protein was in 0.1 M Tris, 0.05 M NaCl, pH 7.8.

dichroism (Anfinsen et al., 1972; Shortle & Meeker, 1986), can be approximated by a two-state model when it is denatured by GuHCl. The mutant is less stable than the wild type, which has a middle point of transition at 0.83 M GuHCl (Shortle & Meeker, 1986) when no ligands are present.

The fluorescent decay of tryptophan in the unlabeled K78C can be adequately represented by two exponentials up to a GuHCl concentration of 0.4 M in the absence of $CaCl_2$ and pdTp, and up to 0.8 M in the presence of the ligands. The lifetimes of the two components in the native protein are about 5.9 and 3.8 ns, and their amplitudes are about 60% and 40% (since the two lifetimes are close, their percentage amplitudes may vary depending on conditions). These lifetimes are very similar to those of wild-type staphylococcal nuclease, indicating that Trp 140 in the mutant is in an environment very similar to that of tryptophan in the wild type. We attribute the two lifetimes solely to the emission from the single tryptophan for the following reasons. We excited the protein at 295 nm and detected at 350 nm, thereby minimizing the absorption due to tyrosine. More importantly, when we measured the fluorescence decay of a mutant nuclease that contains no tryptophan (W140H, where a histidine is substituted for the tryptophan), we did not observe any lifetimes of this mutant that are similar to those of tryptophan at 350 nm. The decay due to tyrosine (λ_{ex} = 280 nm, λ_{em} = 315 nm) was multiexponential and the longest component was ~4.2 ns (James and Brand, unpublished results).

At higher GuHCl concentration, three exponentials are required to fit the data. The average lifetimes (amplitude averaged) show a transition following the denaturation of the protein, as shown in Figure 1B. The average lifetimes under various conditions are shown in Table I. The protein in the presence of Ca^{2+} and pdTp is denatured at a higher GuHCl concentration, consistent with the results of other denaturants (Cuatrecasas et al., 1968). The midpoints of transition for

Table I: Average Parameters from Multiexponential Analysis[a]

	no pdTp (Ca^{2+})				pdTp (Ca^{2+})			
[GuHCl] (M)	$\langle\tau_D\rangle$ (ns)	$\langle\tau_{DA}\rangle$ (ns)	E%	$\bar{r}$ (Å)	$\langle\tau_D\rangle$ (ns)	$\langle\tau_{DA}\rangle$ (ns)	E%	$\bar{r}$ (Å)
0.	5.06	2.59	49	23.0	4.99	2.56	49	23.0
0.20	5.08	2.58	49	23.0				
0.38	4.85	2.46	49	23.0	5.02	2.71	46	23.4
0.61	3.57	2.30	35	22.2	4.98	2.75	45	23.6
0.84	2.46	1.93	22	22.4	4.88	2.62	47	23.3
1.01	2.30	1.82	21	22.6				
1.09					4.04	2.52	38	22.0
1.32					2.72	1.98	32	20.5
2.0	2.12	1.90	10	26.1	2.10	1.80	14	24.5

[a] All average lifetimes were calculated using $\langle\tau\rangle = \sum_i \alpha_i\tau_i$.

the protein with and without ligand binding are about 0.6–0.7 and 0.9–1.0 M.

Denaturation of Labeled K78C in the Absence of pdTp and *Calcium*. The fluorscence decays of tryptophan in K78C with the labeled acceptor IAEDANS were analyzed to obtain average lifetimes using eq 1 and distance distribution information using eq 2. From the average lifetimes of tryptophan in the absence ($\langle\tau_D\rangle$) and presence ($\langle\tau_{DA}\rangle$) of acceptor, the average energy-transfer efficiencies and therefore the average distances under native and denaturing conditions were then calculated. The results are shown in Table I. In the native state, the average distance between tryptophan 140 and cysteine 78 is ~23 Å. For comparison, the distance between tryptophan 140 and lysine 78 of the wild-type nuclease is about 23–25 Å from X-ray data. Thus the overall dimension of the protein as determined from our resonance energy-transfer measurements in solution is in agreement with that from X-ray data. The extension to the size estimation of the nuclease in the denatured state is straightforward. From the data in Table I, the size of the denatured K78C is comparable with that of the native protein. Thus, the denatured state of K78C is quite compact.

We now investigate the distance distribution aspects in the protein. We establish that there is an "apparent" distribution of distances, designate the lifetime of donor-only as τ_D and that of donor–accepted as τ_{DA} (obtained by multiexponential analysis, cf. eq 1, and define the amplitude-weighted lifetime as

$$\langle\tau\rangle_A = \sum_I \alpha_i\tau_i$$

where α_i's are the normalized amplitudes, and intensity-weighted lifetime as

$$\langle\tau\rangle_I = \sum_i \alpha_i\tau_i^2 / \sum_i \alpha_i\tau_i$$

then the ratio $A = \langle\tau_{DA}\rangle_I/\langle\tau_D\rangle_I$ should be equal to the ratio $B = \langle\tau_{DA}\rangle_A/\langle\tau_D\rangle_A$ if there is a single separation distance between the donor and acceptor. A ratio of $A/B > 1$ indicatesa distance distribution (Albaugh et al., 1989). For the native protein K78C, the ratio of A/B is ~1.4. Thus the distribution approach to the distance between Trp 140 and Cys 78 is reasonable.

We used eqs 2 and 3 to obtain a distance distribution between donor and acceptor. A typical fit is shown in figure 2. One symmetric Gaussian distance distribution (cf. eq 3) is sufficient to describe the data. The average distance from the distance distribution fit is ~23 Å, again agreeing with the overall dimension of the wild-type nuclease from X-ray data. The width of the distance distribution is on the other hand quite large for the protein. The standard deviation of the apparent distribution is 7.4 Å, corresponding to a full width at half-maximum height of ~17.6 Å. Protein conformational heterogeneity, orientational factor, and the length of the linker arm all may contribute. We first show that our data are accurate enough to give a unique solution of $\bar{r}$ and σ in eq 3. Similar to the procedures used by others (Lakowicz et al., 1988; Albaugh & Steiner, 1989) with the extension that we also examine the autocorrelation of the residuals, we fix one parameter, σ or $\bar{r}$, while minimizing the reduced χ^2 to test the sensitivity of the optimized parameters. Even 2 Å off the optimal apparent fwhm leads to a large χ^2, and the autocorrelation traces show that all values of apparent fwhm other than the optimal one give poor fit to the data (results not shown). The large value of apparent fwhm is not due to the inability of our instrument to resolve smaller half-widths since we can get as narrow as 1.5 Å in fwhm in triantennary glycopeptides (Rice et al., 1991; Wu et al., 1991).

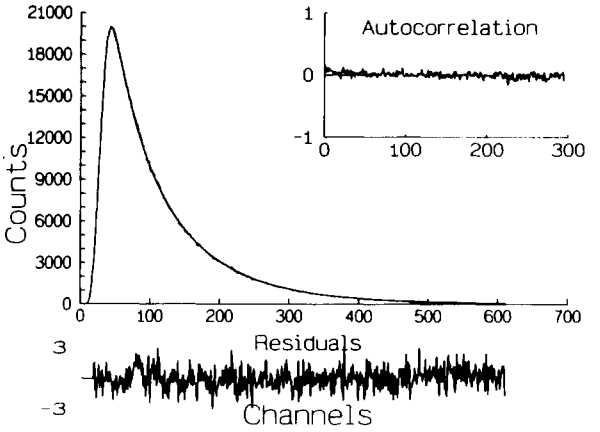

FIGURE 2: Measured and fitted fluorescence decays of Trp 140 in the IAEDANS-labeled staphylococcal nuclease K78C in the native state. The fit was obtained by using eqs 2 and 3 with one-distance distribution. The weighted residuals are shown at the bottom. Autocorrelations of the residuals are shown in the inset. Data were collected at 0.042 ns per channel at 20 °C; excitation 295 nm, emission 350 nm.

The question of discrete distances vs a distribution of distances is addressed further as follows. In the data analysis using eq 2, we fixed the width(s) of the distance distribution(s) to be at 0.1 Å. Thus each distance distribution could be regarded as at a discrete distance (which was yet to be found). We then optimized the relative concentration and average distance of each distribution. The fits with one, two, and three discrete distances are shown in Figure 3. The fit with one discrete distance is very poor, as expected. A two discrete distance fit gives substantial improvement in the quality of fit but the fit is still not optimal. With three discrete distances, the fit is practically the same as that from a distance distribution (cf. Figure 2). At this level, the data do not discriminate between the two models. On the other hand, it

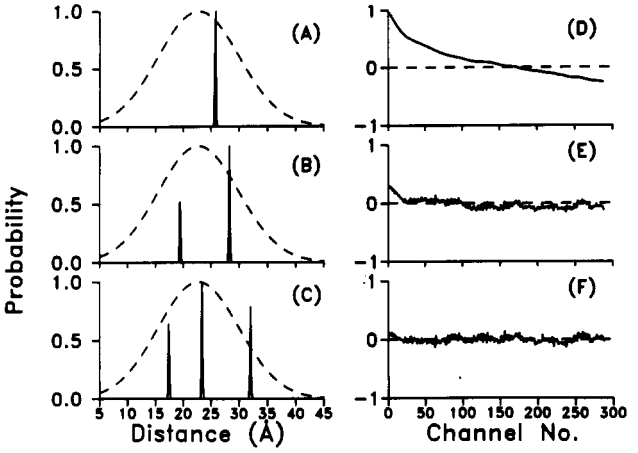

FIGURE 3: Analysis of K78C data in the native state by discrete distances. Fits with one (A), two (B), and three (C) discrete distances. The peak is related to the relative concentration (normalized with respect to the largest population). The dashed line in each plot is the fit by a continuous distance distribution as in Figure 2. The autocorrelations of the fits with one (D), two (E), and three (F) discrete distances are also shown. The corresponding reduced χ^2 are 38.5 in (A), 1.61 in (B), and 1.22 in (C).

is unlikely the protein exists at three discrete distances. Furthermore, the three discrete distances can be viewed as a representative of a continuous distance distribution. Thus, the use of a distance distribution is preferred.

Tryptophan fluorescence decay is complex in most cases (Beechem & Brand, 1985) and only in a few examples does it show single-exponential behavior. We show that even though there is a distribution of lifetimes, its contribution to fwhm of distance distribution in fluorescence energy-transfer measurements is negligibly small when properly handled. For example, a Gaussian lifetime distribution with a mean lifetime of 5 ns and a fwhm of 2.5 ns can be analyzed by two exponentials: $\alpha_1 = 0.4$, $\tau_1 = 3.7$ ns, $\alpha_2 = 0.6$, and $\tau_2 = 5.9$ ns (though larger widths requires more exponential terms). These are very close to the parameters of tryptophan fluorescence in the nuclease in the native state. We used simulated data to determine the contribution to observed distance width from lifetime distribution. In the simulation, we used a Gaussian lifetime distribution ($\bar{\tau} = 5$ ns and fwhm = 2.5 ns) and a single distance at $\bar{R}_0/r = 1$. R_0^6 corresponding to lifetime τ was scaled to be proportional to τ in the distribution of lifetimes. Both simulated data with and without energy transfer were then convoluted with the instrument response by fast Fourier transform, and Poisson noise was added to mimic the experimental data (Wu et al., 1987). In the data analysis, we used the two exponentials of above and a distance distribution exactly the same way as we analyzed the experimental decay data of nuclease. We recovered no more than 1 Å in the apparent fwhm of distance distribution and the fit was very poor. Thus the effect of lifetime distribution can be ignored in our data analysis. The sixth-power dependence of quenched lifetime on the donor–acceptor distance dominates the distance determination. Furthermore, the distance distribution is obtained relative to the lifetimes of the donor (cf. eq 2). The nature of lifetime heterogeneity itself is not important. Therefore, the large apparent fwhm of distance distribution in the nuclease is not due to the heterogeneity of tryptophan fluorescence lifetimes.

The distance resolution by energy-transfer measurements was assessed by analysis of simulated data and experimental data as follows. We used simulated decay data generated with lifetime τ and $\tau/2$ (both single exponential). The decay curve with lifetime $\tau/2$ can be regarded as a decay of donor in the presence of acceptor at a single distance $R_0 = r$. In the data analysis, we used a donor lifetime τ and a Gaussian distance distribution to see how wide a distance distribution could be obtained from a single-distance input. The simulated decay can be fit by a Gaussian with fwhm up to 1.2 Å with very small deviation in the autocorrelation. At about the same degrees of deviation, fwhm obtained from a single-distance input is slightly larger for $r > R_0$ and smaller for $r < R_0$. The resolution was also checked by analyzing experimental data. We measured the fluorescence decay of melatonin, which has a single-exponential lifetime of ~5.4 ns. In the data analysis, we assume that its lifetime was 10.8 ns and the 5.4 ns was due to an "acceptor" quenching at a single distance $r = R_0$. With a Gaussian form, we could obtain fwhm up to 1.5 Å without significant deviation in the autocorrelation. Thus the uncertainities in full width associated with the data analysis are ~ 1.5 Å.

We used $\kappa^2 = {}^2/_3$ to obtain distance distributions. This effectively forces any static orientation into the distance distribution (though both represent heterogeneity). In staphylococcal nuclease, static orientational heterogeneity may exist, as shown in recent work by others. 2D NMR data of wild-type staphylococcal nuclease by Kay et al. (1989) show that there are several disordered regions along the peptide backbone. One region is around Trp 140. Phosphorescence of tryptophan in proteins has been shown to be sensitive to environment and rigidity of the surrounding atoms or molecules. Flexible regions lead to diminishing phosphorescence intensity of tryptophan at room temperature in solution (Strambini & Gonnelli, 1985; Papp & Vanderkooi, 1989). Temperature-dependent studies of tryptophan phosphorescence in staphylococcal nuclease show that Trp 140 in the protein exhibits virtually no phosphorescence at room temperature in solution (Strambini & Gabellieri, 1990). We have tried to observe phosphorescence of Trp 140 of K78C at room temperature under deoxygenated conditions and were unable to get detectable signals. At the present time we cannot exclude other unknown mechanisms, but this may indicate that Trp 140 is flexible on the time scale of phosphorescence (microsecond and longer). On the other hand, fluorescence studies with wild type have shown that (1) tryptophan is somewhat buried in the native state since its fluorescence intensity decreases upon protein unfolding and its fluorescence is not significantly quenched by KI and (2) the tryptophan is rigidly confined since its motion as determined by nanosecond fluorescence anisotropy almost mimics the global motion of the protein. Thus it appears that tryptophan in staphylococcal nuclease is rigid on a short time scale (fluorescence) and flexible on a long time scale (phosphorescence and NMR). Flexibility on a long time scale can lead to heterogeneity in conformation and therefore distance distributions as determined on the nanosecond time scale. Thus distance distribution from fluorescence energy transfer may be regarded as the instantaneous "static" picture of the protein in solution. The potential contribution of the orientational factor to the width of a distance distribution can be estimated according to (Dale et al., 1979; Steiner, 1990)

$$\kappa_{max}^2 = ({}^2/_3)(1 + d_A + d_D + 3d_A d_D) \quad (7)$$

$$\kappa_{min}^2 = ({}^2/_3)(1 - (d_A + d_D)/2) \quad (8)$$

where d_D and d_A are the fractional depolarizations of donor tryptophan and acceptor IAEDANS due to local motions. d_D

is estimated to be 0.96–1.0 and d_A is estimated to be 0.60. For an average distance of 23 Å, an upper limit of 10 Å in the distribution width could be due to orientation. Orientation, however, cannot be the dominant factor since it (Wu & Brand, 1992) would skew the apparent distance distribution shape to longer distances (the apparent distance distribution of K78C–IAEDANS is symmetric).

There are nine single bonds between the α-carbon of cysteine 78 and the acceptor fluorophore. For a linker arm of this length, 8–9 Å in fwhm could be accounted for by its flexibility (Haas et al., 1988). The exact contribution from this factor is difficult to estimate since we have only partial knowledge of the distribution of the acceptor. The fluorescence of IAEDANS is very sensitive to environment, and a large spectral shift occurs from aqueous solution to other conditions (Hudson & Weber, 1973). The denaturation of the nuclease produced no spectral shift, indicating the acceptor is not buried inside the protein. The anisotropy of IAEDANS associated with the protein motion changed little from the native state to the denatured state. Thus the distribution of the acceptor may be only limited by the protein surface and the length of the linker arm. We emphasize that the apparent half-width was obtained by fitting the measured data with a Gaussian form distance distribution. Different model functions may produce different results. For example, the decay data of the native K78C could also be fit with a Lorentzian distance distribution with a half-width of ~11 Å (standard deviation 5 Å), which still implies significant heterogeneity. For proteins in the native states, no theoretical models are available to describe the distance distribution between the two distal sites. The choice of one model over another is somewhat arbitrary. On the other hand, if a protein is totally unfolded to become a random coil, the distance distribution can be approximated as a Gaussian. The use of a Gaussian distance distribution model is preferred so that a systematic comparison is possible. The interpretation of the exact shape of the distance distribution thus should be carried out with caution. The Förster distance used here is 22.8 Å, which is the most sensitive region where energy transfer can be detected. The sixth-power dependence of transfer rates on distance renders estimation of population below or around 16 Å unreliable, due to the high quenching of donor fluorescence at these distances and due to the presence of donors with much less quenching at longer distances. The contributions to half-width of a distance distribution fit from the linker arm can be reduced by selecting probes with shorter linker arms.

The data of K78C at all GuHCl concentrations (up to 2 M) were analyzed by one population of distance distribution with reduced χ^2 between 1.0 and 1.6, random residuals, and random autocorrelations. The average distance and half-width as a function of GuHCl are shown in Figure 4a. As GuHCl increases, the average distance remains constant up to the concentration where the protein is denatured. At higher GuHCl concentration, the average distance increases. The half-width, on the other hand, almost mimics the denaturation of the protein. It stays constant as GuHCl increases and shows a transition as the protein is denatured. But instead of going up as normally expected, it goes down to about half of that in the native state. At higher GuHCl concentration, the half-width goes back again to a higher value. The shape change is quite large as the nuclease is denatured and further unfolded. We also measured one sample at 5 M GuHCl; the energy-transfer efficiency was about 3–5%, which was not accurate enough to obtain a distance distribution but did

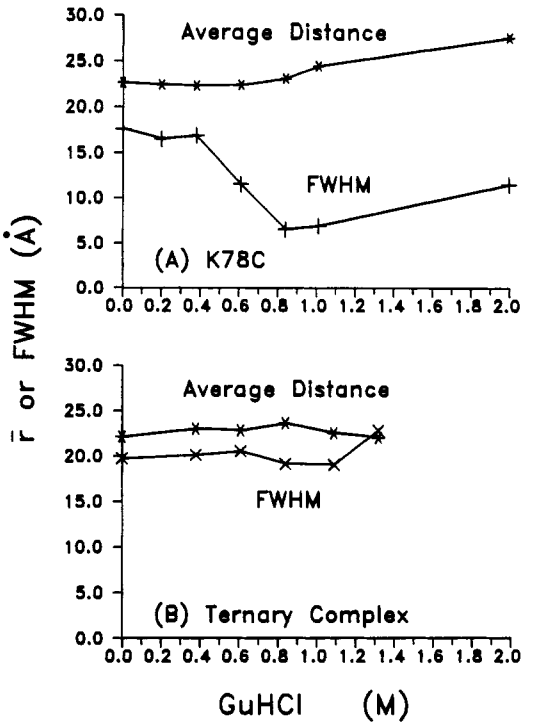

FIGURE 4: (A) Average distance and apparent fwhm of K78C without calcium and pdTp binding vs GuHCl concentration. One Gaussian fit was used at all conditions. The uncertainties with the average distances are about 1–2 Å. (B) Average distance and apparent fwhm of the ternary complex of K78C with calcium and pdTp vs GuHCl concentration. One Gaussian fit to all the data was used up to 1.3 M. The uncertainties associated with the fwhm in the native state are ~2 Å and in the denatured state about 3–4 Å.

indicate a larger distance between the donor and acceptor (greater than 32 Å).

After denaturation, we checked the sample by absorption. It was fully labeled, indicating no detectable decomposition had occurred during our experiments. We also checked the renatured protein after dialyzing the GuHCl out. More than 90% of the fluorescence decay in the sample showed almost identical lifetimes and amplitudes as the native protein. Less than 10% of the signal exhibited a decay with a lifetime of 1 ns. It is not clear whether the small fraction was due to the handling of several steps in dialysis or due to the protein itself.

Denaturation of Labeled K78C in the Presence of pdTp and Calcium. The binding of Ca^{2+} and pdTp stabilizes the mutant of K78C against GuHCl denaturation (Figure 1). Similar to the case of K78C without bound ligands, the fluorescence decays of tryptophan in the ternary complex were analyzed to obtain average lifetimes using eq 1 and distance distribution information using eq 2. The average distances between tryptophan 140 and cysteine 78 in the ternary complex were then calculated under native and denaturing conditions. The results are shown in Table I. In the native state, the average distance is the same as that of the ligand–free nuclease. Thus the binding of ligands produces no significant overall conformational changes though some local changes may occur (Cuatrecasas et al., 1968; Tucker et al., 1979). When the ternary complex is denatured, the size of the denatured state is again comparable with that of the native complex. Therefore the denatured state of the ternary complex is likewise compact. With distance distribution analysis, we can compare the heterogeneity of the denatured protein in the absence and presence of ligands.

The average distance of the ternary complex of nuclease with Ca^{2+} and pdTp is similar to that of the free nuclease in

the native state. The half-width is only ~2 Å larger, an insignificant difference compared to the large values of half-width of the protein with and without ligand binding. When the ternary complex is denatured, a different phenomenon emerges, as shown in Figure 4B. While the average distance remains essentially the same as in the case of the nuclease without ligand binding, the half-width also stays almost the same and then increases instead of decreasing (cf. Figure 4A). At 1.3 M GuHCl, the half-width is equal to the average distance itself.

At 2 M GuHCl, the decay data of the ternary complex show an even greater difference from that of the free nuclease. One Gaussian population fit gave an inadequate fit. We have also tried one Gaussian fit with an asymmetry factor and Lorentzian fit. None of them gave satisfactory fits. Two populations were required to fit the data. The fit with two Gaussians produced satisfactory fits similar to that in Figure 2. The parameters for the first population (cf. eq 2) are $a_1 = 0.33$, $\bar{r} = 15.5$ Å, and $\sigma_1 = 3.9$ Å, and those of the second population, $\alpha_2 = 0.67$, $\bar{r}_2 = 41.6$ Å, and $\sigma_2 = 2.7$ Å. Since the second population is at a large distance where almost no energy transfer occurs, the values of $\bar{r}_2$ and σ_2 are estimates only. a_2 is reliable since it is only related to the fluorescence intensity of the almost unquenched species. The fluorescence lifetime of the donor alone at this GuHCl concentration was quite short (Figure 1) compared to that in the native state. Consequently the signal to noise ratio deteriorated proportionally. The exact shapes of the two populations should be regarded as rough estimates. Nonetheless, compared with the shape changes of the nuclease without ligand binding, there are some effects due to Ca^{2+} and pdTp binding in the denatured states.

In the ternary complex, we observed one very wide distance distribution when the protein was denatured at 1.3 M GuHCl while two populations seemed to be required at 2 M GuHCl. These are the minimal number of parameters needed to describe the data. Physically it is possible that the one wide population might be the superposition of two close distance distributions. We tried with a two-population fit; the results were not unique (in a sense we were overfitting the data) but the two populations by different trials in the initial input of the fit tended to be clustered around 17 and 28 Å, which might be the precursors of the two populations at higher GuHCl. There were no improvements in the reduced χ^2, nor in residuals and the autocorrelation of the residuals. The residuals and the autocorrelation of the residuals were already random with a one-distance distribution fit. Thus, statistically we do not have any basis to go beyond a one-population fit at 1.3 M GuHCl. The decay data at this concentration does not discriminate between a one-population fit and a two-population fit.

DISCUSSION

The average distance from donor Trp 140 to acceptor IAEDANS at position 78 was found to be about the same for the nuclease with and without Ca^{2+} and pdTp binding and it agrees with that from crystallographic data (about 23–25 Å). Even the widths of the distance distribution are very similar. Thus the overall features of the protein do not change much upon Ca^{2+} and pdTp binding. The apparent full width at half-maximum height of the distance distribution is on the other hand quite large. The half-width we observed for the tryptophan–IAEDANS pair is ~18 Å with a Gaussian form distance distribution. This is in the upper range of the measured half-widths for several proteins (Amir & Haas, 1986; Haas et al., 1988; Lakowicz et al., 1988; Albaugh & Steiner, 1989). Since protein conformational heterogeneity, orientation factor, and probe linker arm all may contribute, the present probe provides limited information on the conformational flexibility of the nuclease in the native state. In the denatured state, the partial or total loss of secondary and tertiary structures in proteins leads to a large increase in conformational heterogeneity that dominates the overall observed heterogeneity. Distance distribution analysis provides useful information about the denatured states.

Within the uncertainties of the experiments (1–2 Å), there are essentially no changes in the average distances between Trp 140 and IAEDANS at position 78 as the protein is denatured in the free nuclease and its ternary complexes (cf. Figure 4). Thus *the structure of the nuclease in the denatured state is unlikely to be a random coil.* For comparison, the end to end distance of a random coil of 62 residues (Trp 140–Cys 78) would be (Tanford, 1968) $\langle L^2 \rangle = 60\, n = 60 \times 62$, and $\langle L \rangle \sim 60$ Å for an unperturbed chain. Even with the consideration of nonideal solution, the distance of a random coil should be much larger than the observed distance. Therefore the denatured state is still very compact. It expands only when it is further unfolded at higher denaturant concentrations. Our results with a different acceptor labeling where the linker arm is limited to one or two bonds also confirm the compactness of the denatured state (Wu and Brand, unpublished results). The results of a compact denatured state are consistent with gel filtration studies of nuclease (Shortle & Meeker, 1989).

In the case of free nuclease, the half-width of distance distribution between Trp 140 and IAEDANS at 78 decreases substantially as the protein is denatured (Figure 4A). The decrease of the half-width in the denatured state could be due to several factors. The disorientation of Trp 140 can partly bring down the half-width. The contribution from protein flexibility is 2-fold. If the degree of change in flexibility is larger, such as from a globular protein to a random coil, then the observed half-width should be larger, as it is the case at higher GuHCl concentration (Figure 4A). Diffusion may reduce half-width but not dominate the measurement for such a long peptide. If the degree of change in flexibility is small, then the linker arm of the acceptor may find more accessible space to diffuse, thus reducing the half-width without significantly altering the average distance.

While the binding of Ca^{2+} and pdTp does not change the compactness of the denatured states, the effect on the heterogeneity of the ternary complex is different. The half-width increases as the protein is denatured. In the denatured state, the distribution width of the ternary complex is much larger than that of the free nuclease. To produce such a large difference between free nuclease and its ternary complex, either Ca^{2+}, pdTp, or perhaps both ligands are required to be associated with the nuclease even though the protein is denatured. It has been established by Anfinsen and co-workers (Cuatrecasas et al., 1967) that inhibitor binding requires calcium in the native state. It is not clear whether this can be applied to the denatured state. It is possible that different binding modes, such as weak associations among lysines of the protein, pdTp, and calcium, might produce a more heterogeneous denatured state since the overall dimension of the denatured state is quite compact (Table I and Figure 4B).

Even after the denaturation of the nuclease, the presence of Ca^{2+} and pdTp still produces different results. The nuclease without ligand binding continues to expand. Its average distance increases from ~22 Å of the native state to ~28 Å.

This is probably due to the further unfolding of the protein to gradually become a random coil. At 2 M GuHCl, a one-population fit is still sufficient to represent the data. A two-population fit gave two overlapping populations and the superposition of the two was very close to that of a one-population fit. It is generally accepted that proteins in 6 M GuHCl are close to random coils (Tanford, 1968). At lower GuHCl concentrations, what the structures of proteins look like have not been fully characterized and they may well vary from protein to protein. Results from heme proteins by steady-state energy transfer showed that there are residual structures when the proteins are denatured by GuHCl (Tsong, 1975). In our case the protein is denatured at quite low GuHCl concentrations in which residual structures may be expected, and it appears that the nuclease may still possess residual structures or the hydrophobic cores are not completely disrupted up to 2 M GuHCl.

ACKNOWLEDGMENT

We thank Dr. D. Shortle of the Department of Biological Chemistry, The Johns Hopkins University, for providing the mutant clones of staphylococcal nuclease in this study and reading of the manuscript. We thank Dr. R. P. De Toma of the Department of Chemistry of Loyola College, Baltimore, MD, for data aquisition automation hardware and software and helpful advise.

REFERENCES

Albaugh, S., & Steiner, R. F. (1989) *J. Phys. Chem. 93*, 8013–6.
Albaugh, S., Lan, J., & Steiner, R. F. (1989) *Biophys. Chem. 33*, 71–6.
Amir, D., & Haas, E. (1986) *Biopolymers 25*, 235–40.
Anfinsen, C. B. (1973) *Science 181*, 223–30.
Anfinsen, C. B., Schechter, A. N., Taniuchi, H. (1972) *Cold Spring Harbor Symp. Quant. Biol. 36*, 249–55.
Badea, M., & Brand, L. (1979) *Methods Enzymol. 61*, 378–425.
Beechem, J., & Brand, L. (1985) *Annu. Rev. Biochem. 54*, 43–71.
Beechem, J., James, E., & Brand, L. (1990) *Proc. SPIE, 1204*, 686–98.
Cuatrecasas, P., Fuchs, S., & Anfinsen, C. B. (1967) *J. Biol. Chem. 242*, 1541–7.
Cuatrecasas, P., Taniuchi, H., & Anfinsen, C. B. (1968) *Brookhaven Symp. Biol. 21*, 172–200.
Dale, R. F., Eisinger, J., & Blumberg, W. E. (1979) *Biophys. J. 26*, 161–94.
Ellman, G. L. (1959) *Arch. Biochem. Biophys. 82*, 70–7.
Fuchs, S., Cuatrecasas, P., & Anfinsen, C. B. (1967) *J. Biol. Chem. 242*, 1768–70.
Gill, S. C., & von Hippel, P. H. (1989) *Anal. Biochem. 182*, 319–26.
Grinvald, A., & Steinberg, I. Z. (1974) *Anal. Biochem. 59*, 583–98.
Haas, E., Wilchek, M., Katchalski-Katzir, E., & Steinberg, I. Z. (1975) *Proc. Natl. Acad. Sci. U.S.A. 72*, 1807–11.
Haas, E., McWherter, C. A., Scheraga, H. A. (1988) *Biopolymer, 27*, 1–21.
Hudson, E. N., & Weber, G. (1973) *Biochemistry 12*, 4154–60.
Kay, L. E., Torchia, D. A., & Bax, A. (1989) *Biochemistry 28*, 8972–9.
Kirby, E. P., & Steiner, R. F. (1970) *J. Phys. Chem. 74*, 4480–90.
Lakowicz, J. R., Gryczynski, I., Cheung, H. C., Wang, C. K., Johnson, M. L., & Joshi, N. (1988) *Biochemistry 27*, 9149–60.
Papp, S., & Vanderkooi, J. M. (1989) *Photochem. Photobiol. 49*, 775–84.
Rice, K. G., Wu, P. G., Brand, L., & Lee, Y. C. (1991) *Biochemistry 30*, 6646–55.
Serpersu, E. H., Shortle, D., & Mildvan, A. S. (1986) *Biochemistry 25*, 68–77.
Shortle, D. (1989) *J. Biol. Chem. 264*, 5315–8.
Shortle, D., & Meeker, A. K. (1986) *Proteins: Struct. Funct. Genet. 1*, 81–9.
Shortle, D., & Meeker, A. K. (1989) *Biochemistry, 28*, 936–44.
Shortle, D., Stites, W. E., & Meeker, A. K. (1990) *Biochemistry 29*, 8033–41.
Steiner, R. F. (1990) *Comments Mol. Cell. Biophys. 6*, 385–404.
Strambini, G. B., & Gonnelli, M. (1985) *Chem. Phys. Lett. 115*, 196–200.
Strambini, G. B., & Gabellieri, M. (1990) *Photochem. Photobiol. 51*, 643–8.
Tanford, C. (1968) *Adv. Protein Chem. 23*, 121–282.
Tsong, T. Y. (1975) *Biochemistry 14*, 1542–8.
Tucker, P. W., Hazen, E. E., & Cotton, F. A. (1979) *Mol. Cell. Biochem. 23*, 3–16.
Wu, P. G., & Brand, L. (1992) *Biochemistry 31*, 7939–47.
Wu, P. G., Fujimoto, B. S., & Schurr, J. M. (1987) *Biopolymers 26*, 1463–88.
Wu, P. G., Rice, K. G., Brand, L., & Lee, Y. C. (1991) *Proc. Natl. Acad. Sci. U.S.A. 88*, 9355–9.